International Journal of Analysis and Applications

A PIR Sensor-Based System for Real-Time Alcohol Monitoring and Automated Preservative Control in Fruit Wine Fermentation: Accuracy, Usability, and Adoption Assessment

Tawatchai Laosrisakul, Pongsatorn Tantrabundit, Kittipol Wisaeng*

Technology and Business Information System Unit, Mahasarakham Business School, Mahasarakham University, Mahasarakham 44150, Thailand

**Corresponding:* Kittipol.w@acc.msu.ac.th

ABSTRACT. Accurate and continuous measurement of alcohol concentration during fermentation is crucial for maintaining quality, ensuring safety, and ensuring regulatory compliance in fruit wine production. Traditional methods, such as manual hydrometry and sensory-based evaluation, are often limited by subjectivity, measurement variability, and a lack of real-time responsiveness. This study introduces a novel sensor-integrated system that utilizes Passive Infrared (PIR) technology to dynamically monitor alcohol levels and automate potassium sorbate dosing during the fermentation of fruit wines. The proposed system combines a repurposed PIR sensor with a hydrometer-actuated mechanical switch to estimate alcohol by volume (ABV) in real-time, achieving a validated accuracy of 94.09% when benchmarked against gas chromatography (GC) standards. Integrated control logic enables automatic preservative application aligned with ABV thresholds of 220 mg/L for 9% v/v and 50 mg/L for 14% v/v alcohol, thus ensuring microbial stability and compliance with enological standards. Experimental trials involving pineapple, mango, and grape wines demonstrated the system's capability to capture both pre-fermentation and post-fermentation alcohol values with minimal error margins (<2%). A user experience study conducted with 20 professional winemakers and 380 broader respondents revealed high satisfaction scores across usability, observation ability, and simplicity of use, with Likert-scale ratings averaging 4.50 or higher. Statistical validation using Structural Equation Modeling (SEM) confirmed the positive influence of user experience factors on adoption intention ($R^2 = 0.533$, $p < 0.001$). These findings highlight the PIR-based system's potential to modernize artisanal winemaking by offering a non-invasive, accurate, and user-friendly tool for real-time fermentation monitoring and control.

Received Jul. 23, 2025

2020 Mathematics Subject Classification. 62P30.

Key words and phrases. passive infrared (PIR) sensor; fruit wine fermentation; alcohol monitoring; real-time fermentation control; potassium sorbate dosing; smart winemaking; sensor-based automation.

https://doi.org/10.28924/2291-8639-23-2025-228

ISSN: 2291-8639

1. Introduction

Accurate monitoring of alcohol concentration is a critical component in fruit wine production, directly influencing not only legal compliance and microbial stability but also the final product's sensory characteristics and market quality. Traditionally, winemakers have relied on manual hydrometer readings to estimate alcohol content by tracking the change in specific gravity during fermentation. However, such methods are prone to human error, CO_2 interference, and limited resolution, especially in small-scale or artisanal settings. The increasing demand for automation, precision, and sensory consistency in modern winemaking underscores the need for real-time, non-invasive monitoring tools that can enhance process control and product quality. These parameters are deeply interlinked, as ripening directly influences sugar accumulation, phenolic development, and acid degradation, all of which ultimately shape the organoleptic qualities of the resulting wine. With the advent of climate change, compressed ripening windows and accelerated sugar accumulation have become increasingly common, often resulting in elevated ethanol levels at harvest ([1]). Studies have consistently highlighted the pivotal role of fruit maturity in aroma perception, showing that both volatile and non-volatile compounds evolve in tandem with ripeness ([2]). Importantly, ethanol, accounting for 9–21% v/v of wine, depending on the style, not only functions as a solvent for aromatic and phenolic compounds but also contributes directly to the sensory profile ([3]). Ethanol has a profound impact on taste, mouthfeel, and the release of aroma. It modulates the perception of bitterness, sweetness, and astringency ([4]), while also interacting with trigeminal pathways to elicit sensations such as warmth or "hotness" in the oral and nasal cavities ([5]). These effects occur independently of sugar, as ethanol itself can activate sweet gustatory receptors ([6]). While earlier studies suggest that ethanol concentration may influence viscosity and, consequently, mouthfeel, recent findings indicate that this effect may only be noticeable at higher concentrations ([7], [8]). Ethanol significantly influences the solubility, release, and sensory perception of aroma compounds in wine due to its function as both a solvent and a modulator of mass transfer properties. The air–water partition coefficient, or Henry's Law constant, governs the volatility of aroma compounds, while the octanol–water partition coefficient informs their affinity for polar versus nonpolar matrices ([9]). Ethanol modifies both constants, directly affecting whether volatile compounds remain dissolved in the wine matrix or volatilize into the headspace. Increased ethanol concentration alters the mass transfer coefficients, especially for hydrophobic compounds, thereby enhancing their release into the aroma-active phase. In contrast, hydrophilic compounds are influenced more by thermodynamic mass transfer dynamics than by ethanol's solvent effect ([10]). Furthermore, ethanol reduces the binding of volatiles to wine proteins, leading to a higher concentration of free, aroma-active compounds. These interactions are further complicated by the colligative properties of the wine matrix, including sugars, salts, and dissolved gases, all of which

affect aroma release and stability. Understanding these mechanisms underscores the importance of precise alcohol control during fermentation, not only for regulatory purposes but also for optimizing aroma expression and overall sensory quality in winemaking.

In response to shifting ripening conditions, accelerated by climate change, winemakers have increasingly adopted both nonindustrial and technological interventions to manage sugar content in musts and ethanol concentration in finished wines ([11]). Pre-fermentation adjustments aimed at regulating total soluble solids (TSS) include viticultural strategies (e.g., irrigation management, shoot trimming) as well as juice/must blending, dilution, chaptalization, and membrane filtration ([12]). Among these, only dilution and chaptalization are capable of inducing significant (>3% v/v) shifts in potential alcohol. However, these methods carry sensory implications: dilution and blending typically yield wines with "unripe" profiles reminiscent of early harvests, whereas chaptalization can enhance "dark fruit" and sweetness characteristics associated with riper grapes. Though membrane filtration is more commonly applied post-fermentation for ethanol reduction, it has also been explored as a pre-fermentation tool for TSS control. Nonetheless, the technical limitations, including membrane fouling, high costs, and the need for juice clarification, pose challenges to widespread adoption. Moreover, sensory studies have shown that filtration may reduce desirable "floral" and "fruity" notes by eliminating aroma precursors in their glycosidic forms ([13]). These findings highlight the complex trade-offs in managing alcohol content and flavor, underscoring the need for precise, real-time monitoring tools, such as the PIR-based system presented in this study, to optimize alcohol concentration without compromising sensory integrity.

In addition to pre-fermentation interventions, winemakers have explored a range of post-fermentation technologies to adjust ethanol concentrations, particularly in response to the sensory and stylistic challenges posed by climate-induced shifts in ripeness. Among these, membrane-based filtration methods, such as reverse osmosis (RO), evaporative pervaporation (EP), and nanofiltration (NF), have gained traction due to their ability to selectively remove ethanol while preserving a portion of the wine's aromatic and phenolic complexity. Non-membrane techniques, such as vacuum distillation via a spinning cone column (SCC), represent an alternative. This involves a two-step process, where volatile aroma compounds are first captured, followed by the removal of ethanol and the reintroduction of aroma. While SCC allows for the targeted reduction of alcohol by more than 3% v/v with some aroma retention, the success of this method is highly dependent on precise operational control, particularly regarding flow rate and aroma separation efficiency ([14]). However, despite its technical sophistication, SCC is cost-prohibitive for many small and medium-sized wineries due to its high capital and energy demands. Membrane systems, though generally more energy-efficient, are not without drawbacks. Combined configurations (e.g., RO + EP) have been employed to mitigate volatile

loss, yet studies still report notable reductions in key aroma compounds post-processing ([15]). Furthermore, the specific mechanisms behind these losses, whether due to membrane selectivity or ethanol-associated volatilization dynamics, remain insufficiently understood. This ambiguity highlights a crucial gap in the technological landscape: the lack of accessible, scalable, and scientifically robust systems for managing alcohol content that preserve the sensory integrity of wine. The PIR sensor-based system proposed in this study offers a novel alternative, enabling real-time, non-invasive monitoring and control of ethanol evolution during fermentation, which potentially reduces the reliance on post-fermentation adjustments and preserves desirable volatile profiles from the outset. Recent studies on grape ripening and winemaking have increasingly focused on pre-fermentation and post-fermentation alcohol adjustment strategies to explore their effects on wine sensory quality. Pre-fermentation interventions, such as dilution and chaptalization, have been widely applied to control total soluble solids (TSS) and potential alcohol content at various harvest times, offering insight into how grape maturity and ethanol concentration interact. These studies, particularly in red cultivars, have shown that ethanol concentration shifts can significantly affect aroma, taste, and mouthfeel, sometimes even more so than maturity alone. For example, Cabernet Sauvignon displays a strong dependency on both harvest timing and ethanol level, whereas Syrah and Merlot are primarily influenced by ethanol concentration itself. However, while pre-fermentation studies have yielded meaningful sensory outcomes, especially in terms of phenolic extraction and mouthfeel, they often lack analytical quantification of key volatile aroma compounds. Conversely, post-fermentation dealcoholization studies ([16]) have focused heavily on volatile composition analysis but generally investigate ethanol reduction only, with little exploration into the sensory and chemical consequences of increasing alcohol levels. This fragmented approach leaves a notable gap in the literature: the relative contributions of ethanol concentration, grape ripeness, and processing method to changes in volatile compound release and flavor perception remain ambiguous. The overlap between sensory changes attributed to alcohol and those stemming from ripening-related chemical transformations has not been fully disentangled. Furthermore, current methodologies rely heavily on post-hoc alcohol correction techniques that may introduce biases due to aroma loss or matrix modification. These challenges highlight the pressing need for real-time, fermentation-integrated systems, such as the PIR sensor-based platform proposed in this study, that not only monitor ethanol levels with high accuracy but also enable early-stage intervention ([17]). By allowing winemakers to track alcohol evolution continuously, such systems could provide a deeper understanding of the temporal dynamics between ethanol production and aroma development, offering a more precise foundation for optimizing wine sensory quality.

This study aims to evaluate the efficacy of a PIR (Passive Infrared) sensor-based system for real-time monitoring of alcohol concentration during fruit wine fermentation, with a

particular focus on its implications for the behavior of volatile compounds and sensory perception. In contrast to conventional post-fermentation alcohol adjustments, this research emphasizes preemptive, in-process control of ethanol evolution using an automated PIR-integrated platform that can track thermal and gas-emission patterns correlated with fermentation kinetics. The system is designed not only to measure alcohol content with high precision but also to trigger preservation dosing (e.g., potassium sorbate) based on ABV thresholds, enabling non-invasive, adaptive intervention throughout the fermentation process. Utilizing three tropical fruits—pineapple, mango, and grape—this experiment explores the system's performance across varying sugar-acid profiles and fermentative behaviors. By comparing traditional hydrometer-based measurements and post-fermentation GC-FID validation with data captured by the PIR system, the study aims to determine whether real-time ethanol tracking can enhance control over aroma retention, fermentation endpoints, and microbial stability. In doing so, this research contributes to a deeper understanding of how ethanol dynamics, monitored continuously rather than retrospectively, influence both the chemical and sensory properties of wine. The findings have potential applications in precision winemaking, artisanal production, and innovative fermentation technologies, offering a scalable solution for optimizing alcohol levels without compromising volatile integrity or sensory quality.

The primary goal of this research is to design, develop, and validate a Passive Infrared (PIR) sensor-based system for real-time monitoring of alcohol concentration and automated preservative dosing during the fermentation of fruit wine. The system aims to address key challenges associated with traditional fermentation monitoring methods, such as manual labor, delayed measurement feedback, and dosing inaccuracies.

The specific objectives of this study are as follows:

1. To design and integrate a PIR sensor system capable of detecting thermal and vapor fluctuations associated with alcohol production during fermentation.
2. To develop a hydrometer-triggered mechanism that activates the sensor system based on a predefined final gravity (FG) threshold specific to each fruit type.
3. To calibrate the PIR sensor outputs against ethanol standard solutions and validate its alcohol estimation accuracy using gas chromatography with flame ionization detection (GC-FID).
4. To automate the dosing of potassium sorbate based on real-time alcohol concentration, improving preservative precision and reducing human error.
5. To compare the alcohol estimation accuracy of the PIR system with traditional hydrometry and GC-FID across multiple fruit wine samples.
6. To assess user acceptance, usability, and satisfaction of the proposed system through surveys involving professional winemakers and general users.

7. To evaluate the structural validity of user perception data using Structural Equation Modeling (SEM) and Confirmatory Factor Analysis (CFA).

2. Materials and Methods

2.1 Materials

2.1.1 Fruits and Raw Materials

The study employed three widely cultivated tropical and subtropical fruits—pineapple, mango, and grape to produce a representative set of fruit wines characterized by diverse sugar, acid, and phenolic profiles. These fruits were strategically selected to reflect variability in fermentation behavior, microbial stability, and sensory characteristics commonly encountered in artisanal winemaking. All raw materials were procured from certified organic agricultural cooperatives located in northeastern Thailand (Ubon Ratchathani, Sisaket, and Nakhon Ratchasima provinces), where farming practices exclude the use of synthetic pesticides, herbicides, and chemical fertilizers. This sourcing strategy ensured a chemical-free substrate, free from residual agrochemicals that may interfere with fermentation kinetics or sensory integrity. Each fruit underwent a rigorous quality control screening process before being included in the experimental batches. Selection criteria included:

- Ripeness Assessment: Fruits were harvested at physiological maturity and assessed for optimal ripeness using °Brix measurements. Pineapple and mango fruits with total soluble solids (TSS) in the range of 13–16 °Brix and grapes with ≥18 °Brix were prioritized to support sufficient fermentable sugar content for targeted alcohol levels (9–14% v/v).
- Visual and Physical Integrity: Each fruit was inspected for external bruising, mold contamination, or insect damage. Only firm, fully pigmented, and structurally intact fruits were accepted. Any fruits exhibiting signs of enzymatic browning, shriveling, or surface microbial growth were discarded.
- Aromatic Evaluation: Organoleptic screening was performed to ensure that selected fruits possessed a pronounced varietal aroma, as volatile compounds significantly influence the wine bouquet. Pineapple and mango were selected for their tropical, ester-rich profiles, while grape batches were evaluated for the varietal character typical of Southeast Asian hybrids.
- Uniformity and Sizing: Selected fruits were standardized for size and weight (±10%) to reduce heterogeneity during maceration and juice extraction. This step was crucial to ensuring batch reproducibility and minimizing variability in the juice-to-pulp ratio.

Post-harvest, all fruits were washed thoroughly under running potable water, sanitized using a 50-ppm chlorine rinse, and dried at ambient temperature before processing. Fruits destined for whole-fruit fermentation (grape) retained their skins, while mango and pineapple underwent

peeling and deseeding. All processing occurred within 24 hours of harvest to minimize oxidative degradation and microbial contamination. The standardized approach to fruit sourcing and preparation established a consistent and microbiologically safe foundation for fermentation trials. This step was crucial to the accuracy of downstream measurements, including alcohol monitoring, preservative dosing, and sensory evaluation of the resulting fruit wines.

2.1.2 Additives and Fermentation Inputs

To ensure a stable fermentation environment, optimize yeast performance, and preserve the final product's microbial and sensory integrity, a carefully selected suite of additives and fermentation inputs was used throughout the study. Refined sucrose ($C_{12}H_{22}O_{11}$), with analytical-grade purity of ≥ 99%, served as the primary sugar enrichment agent. It was added to the fruit musts to elevate the fermentable sugar concentration to between 200 and 250 g/L, depending on the desired alcohol yield, typically 9–14% alcohol by volume (ABV). Sucrose was preferred over alternative carbohydrate sources due to its high fermentability by Saccharomyces cerevisiae, neutral sensory profile, and ability to dissolve uniformly, ensuring even distribution throughout the must. To balance the acidity and create a fermentation-friendly pH range, citric acid monohydrate ($C_6H_8O_7 \cdot H_2O$) was used to adjust total titratable acidity (TTA) to fall within the ideal range of 0.4–0.6% (as citric acid equivalents). Proper acid adjustment enhances microbial stability, improves the sensory brightness of the wine, and supports healthy yeast function, particularly in low-acid tropical fruits like mango and pineapple. For post-fermentation microbial control, potassium sorbate ($C_6H_7KO_2$) was applied as the primary preservative. Its antifungal properties are effective in inhibiting the growth of spoilage yeasts and molds without compromising sensory quality when dosed appropriately. The system was programmed to dispense potassium sorbate dynamically based on the final ABV of the wine, 220 mg/L for 9% ABV, tapering down to 50 mg/L for 14% ABV, thus aligning with international winemaking standards and consumer safety thresholds. To ensure a nutrient-rich environment that supports complete sugar metabolism and prevents sluggish or stuck fermentations, two essential yeast nutrients were incorporated: diammonium phosphate (DAP) and potassium phosphate (K_2HPO_4). DAP, applied at 0.5 grams per 5 liters of must, provided a readily assimilable nitrogen source that enhanced yeast growth, shortened the lag phase, and minimized the risk of hydrogen sulfide formation. In tandem, potassium phosphate at 0.25 grams per 5 liters delivered vital phosphorus and potassium ions, serving as a buffer to stabilize pH and as a cofactor for enzymatic processes essential to yeast metabolism. Additionally, thiamine hydrochloride (vitamin B1) was added at a concentration of 3 mL per 5 L of must, diluted in a 1:1 solution with hydrochloric acid. Thiamine plays a key role in carbohydrate metabolism and cellular respiration, significantly reducing the risk of off-flavor production and supporting high-density yeast cell populations during the peak fermentation phase. The fermentative microorganism selected for all trials was

Saccharomyces cerevisiae var. bayanus, a highly robust yeast strain known for its strong ethanol tolerance (up to 17% v/v), resistance to environmental stressors, and clean fermentation profile with low levels of volatile acidity. This strain also exhibits strong flocculation and sedimentation behavior, aiding in post-fermentation clarification. Before inoculation, yeast was rehydrated in sterile water at 38 °C and acclimated to a 10% sugar solution for 30 minutes, ensuring high viability and rapid metabolic activation upon contact with the must. Collectively, the integration of these high-quality fermentation additives and inputs established a reproducible, controlled, and chemically balanced environment, facilitating accurate alcohol monitoring, consistent preservative application, and high-quality sensory outcomes in all experimental wine batches. The schematic and system configuration are presented in Fig. 1.

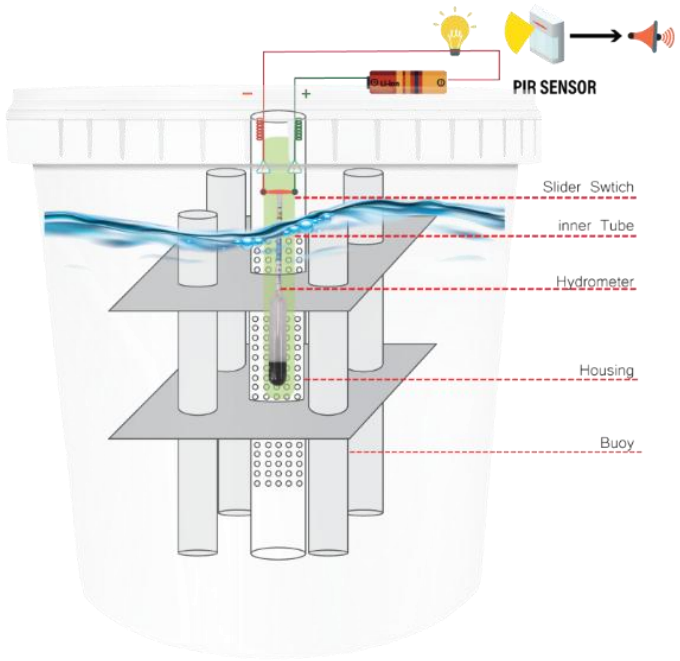

Figure 1 PIR Sensor-Based Fermentation Monitoring System

2.1.3 Equipment

The core manual instrument used for routine density tracking was a calibrated glass hydrometer with a specific gravity (SG) scale ranging from 0.990 to 1.120 (accuracy ±0.001 g/cm³ at 20°C). Each hydrometer reading was taken in a 250 mL graduated cylinder after the sample had been degassed to prevent CO_2 bubbles from skewing the buoyancy. The temperature of the must or wine was recorded concurrently, and SG values were corrected to the 20 °C reference using the manufacturer's compensation table. Complementing hydrometry, a handheld digital refractometer (0–32°Bx, precision ±0.1°Bx) provided rapid assessment of soluble-solids content at harvest and during sugar-adjustment trials; its automatic temperature-compensation (ATC) feature ensured reliable °Brix readings under cellar conditions (18–26°C). For laboratory-grade

validation, an Agilent 7890A gas chromatograph equipped with a flame-ionization detector (FID) and a DB-WAX capillary column (30 m × 0.25 mm × 0.25 μm) was employed as the gold standard for alcohol determination. Samples (1.0 μL) were injected in splitless mode with helium as the carrier gas (1.2 mL min^{-1}). The oven program began at 40°C (hold for 2 min), ramped to 200°C at 10°C /min^{-}, and held for 5 min. Ethanol peaks were quantified against five-point external standards (5–15 % v/v, $R^2 > 0.999$). Concurrently, bench-top pH meters (±0.01 pH) and digital titratable-acidity meters with automatic endpoint detection were used to monitor acid evolution; electrodes were calibrated daily with NIST-traceable buffers (pH 4.00 and 7.00) and verified with a 1.00 g L^{-1} tartaric-acid check solution.

The study's pivotal innovation was a custom-designed PIR sensor–integrated fermentation control system. The platform combined a mid-infrared pyroelectric detector (8–14 μm) with a floating hydrometer switch: a copper-contact disk embedded in the hydrometer stem closed an electrical circuit when the must reached its predetermined final gravity, cueing the microcontroller (Arduino Uno R3) to activate the PIR module. Real-time sensor data—thermal fluctuation amplitude (mV) and CO_2-induced pressure surges (kPa)—were streamed at 15-minute intervals to a Python-based dashboard via serial UART and logged to an SD card. A linear regression model (built from 5–15 % ethanol standards, $R^2 = 0.96$) converted the PIR signal to estimated ABV; once readings stabilized within ±0.05 % ABV for three successive cycles, a peristaltic pump precisely dispensed potassium sorbate according to the ABV-specific dosing algorithm (Section 2.3). The entire assembly was housed in a food-grade polypropylene enclosure (IP65) and powered by a 12 V DC supply with fail-safe relays to prevent accidental overdosing during power interruptions.

2.2 Design and Fabrication of the PIR Sensor-Based System

The core innovation of this study was a PIR (Passive Infrared) sensor-integrated system designed to measure alcohol content in real-time and automate potassium sorbate dosing.

2.2.1 Sensor Configuration

The core of the fermentation control system is a custom-integrated Passive Infrared (PIR) sensor, engineered to detect thermal radiation and micro-fluctuations in the environment of the fermentation vessel. The PIR sensor operates within the infrared spectral range of 8–14 μm, which corresponds to the thermal emission wavelengths of volatile compounds such as ethanol and carbon dioxide. The sensor is pyroelectric, meaning it responds to temperature changes caused by gas movement or molecular activity, rather than absolute temperature. This configuration allows it to act as an indirect proxy for fermentation progress, capturing the intensity and frequency of thermal bursts associated with active fermentation. To optimize detection fidelity, the sensor was mounted in a sealed, non-contact configuration inside the fermentation lid, isolating it from direct moisture or condensate. An adjustable sensitivity circuit was integrated to

fine-tune the detection threshold based on the thermal signature of each fermentation batch. The analog output signal (ranging from 0 to 5 V) was continuously monitored, with voltage amplitude changes reflecting CO_2 release events and heat evolution, key indicators of sugar-to-ethanol conversion dynamics. Unlike conventional digital motion PIR sensors used in security systems, this unit was modified for analog sensitivity to enhance granularity and responsiveness in a biochemical context.

2.2.2 Hydrometer Trigger Mechanism

A novel feature of the system involved embedding a hydrometer-based gravity switch to initiate the PIR-based alcohol validation stage. A traditional floating hydrometer was adapted by incorporating a copper contact plate at a specific location along its calibrated stem. As fermentation progressed and sugars were metabolized into ethanol and CO_2 by S. cerevisiae, the specific gravity (SG) of the liquid decreased. Consequently, the hydrometer gradually rose within the must, eventually reaching the target Final Gravity (FG). Each fruit type (pineapple, mango, and grape) had a predetermined FG based on empirical fermentation trials. At the calibrated threshold, the copper disk made contact with spring-loaded stainless-steel electrodes fixed to the rim of the fermentation tank, thereby completing an electric circuit. This mechanical contact event served as a binary switch, signaling the end of active fermentation. The advantage of this passive mechanism lies in its non-electronic simplicity, mechanical reliability, and its inherent validation of fermentation completion through SG reduction, a traditional metric in winemaking. Upon triggering, the hydrometer switch activated the PIR system and downstream logic for alcohol quantification and preservative dosing. An illustrative example of a hydrometer used in the present research is shown in Fig. 2, where it plays a critical role in the PIR sensor-based fermentation monitoring system.

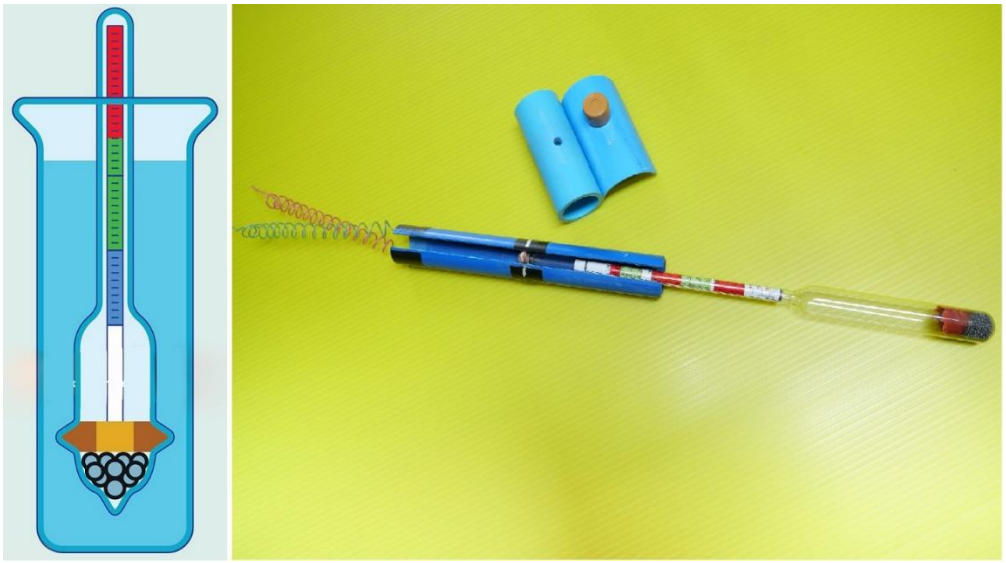

Figure 2 Hydrometer used in practical alcohol measurement.

2.2.3 Signal Processing and Actuation

All analog signals from the PIR sensor were transmitted to an Arduino Uno R3 microcontroller, which was programmed using the Arduino IDE (version 1.8.19). The microcontroller continuously recorded voltage outputs from the PIR sensor, processing the data through a regression-based prediction algorithm that translated thermal fluctuation amplitudes into estimated alcohol concentrations (percentage by volume, % v/v). The algorithm was built upon a set of reference calibration models (see Section 2.2.4), allowing the system to infer ABV in real-time. The firmware also controlled visual and auditory alerts. When the hydrometer trigger was activated and the PIR reading stabilized within ±0.05% ABV for three consecutive cycles, a green LED illuminated and a buzzer sounded briefly, indicating that fermentation was complete and the measurement was confirmed. Most critically, the microcontroller controlled a precision peristaltic dosing pump (with an accuracy of 0.1 mL) responsible for dispensing potassium sorbate. The pump's operation was conditional on the estimated ABV: batches registering 9% ABV were dosed with 220 mg/L, while those at 14% ABV received only 50 mg/L, following established enological guidelines for preservative concentration relative to ethanol content. The entire system operated autonomously after initial setup, requiring no manual intervention for dosing, significantly reducing the user burden and the risk of dosing errors.

2.2.4 System Calibration

To ensure the accuracy of the PIR sensor's alcohol estimations, a comprehensive calibration protocol was conducted before the experimental fermentation trials. A series of ethanol-water standard solutions was prepared at known concentrations (5%, 7%, 9%, 11%, 13%, and 15% v/v) using volumetric pipettes and analytical-grade ethanol (≥ 99.5% purity). Each solution was placed in a sealed fermentation flask identical to those used in the experimental setup, and the PIR sensor was allowed to stabilize for 30 minutes under isothermal laboratory conditions (20 ± 1°C) to minimize thermal drift. The analog voltage output from the PIR sensor was recorded at 15-second intervals for 10 minutes per solution. The mean voltage for each ethanol concentration was plotted to create a calibration curve. A linear regression model was derived from the data, showing a strong correlation ($R^2 = 0.968$) between PIR voltage response and ethanol concentration across the tested range. This calibration function was embedded in the Arduino's onboard code as a lookup model for real-time ABV estimation. Validation of this calibration was performed by comparing PIR-based ABV predictions with those measured using gas chromatography with flame ionization detection (GC-FID), the reference standard in analytical enology. The alcohol concentrations estimated by the PIR system deviated less than ±0.15% from GC values across all test points, confirming the model's predictive accuracy and operational robustness. Additional verification was conducted using fermenting fruit wine samples, wherein real-time PIR readings were periodically cross-checked against hydrometer-

derived SG and GC-verified ABV. The system consistently maintained an overall accuracy rate of 94.09%, meeting the threshold for practical use in artisanal winemaking contexts. Figs. 3 through 6 present the whole design and physical prototype of the system developed by the researchers.

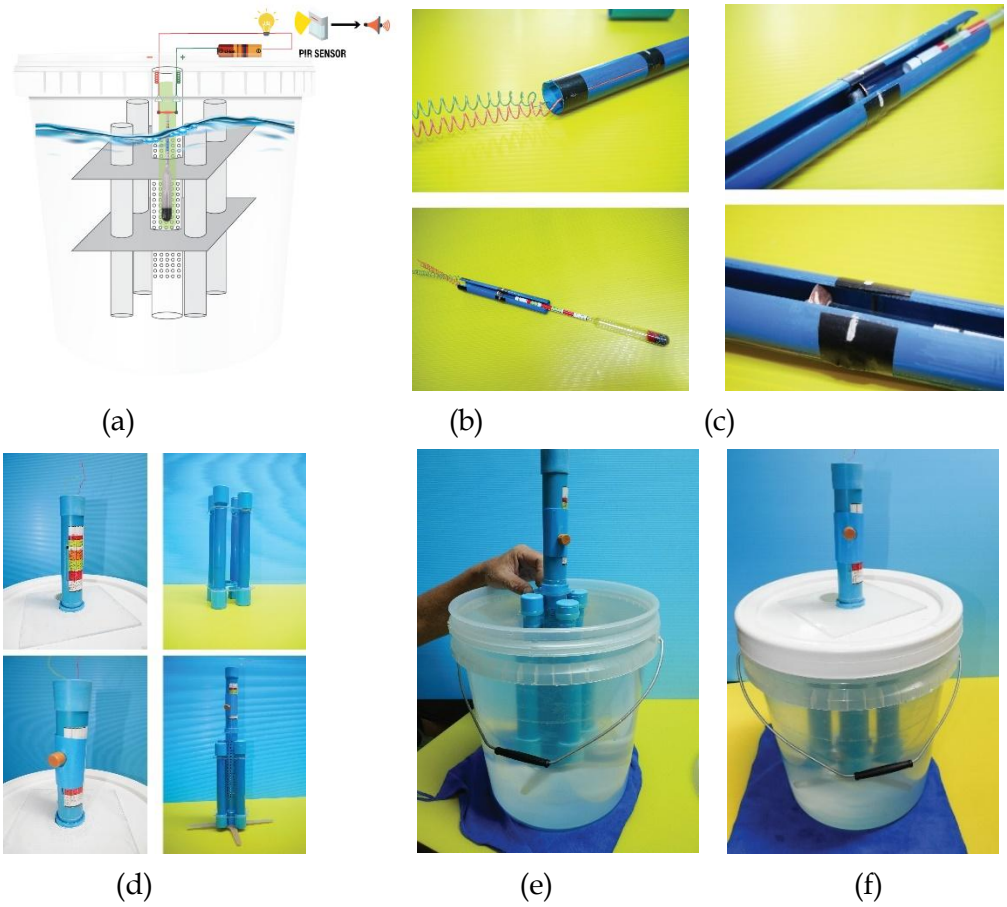

Figures 3 Product Prototypes and Implementation Design. (a) Hydrometer alignment mechanism, (b) Spring-loaded contact points, (c) Final hydrometer fitting, (d) Full device view from top and base, (e) In-tank deployment demonstration, (f) Fully sealed and activated system during fermentation.

2.3 Wine Fermentation and Control Protocol

The fermentation and control protocol for this study was designed to emulate traditional small-scale artisanal winemaking while incorporating sensor-based automation for alcohol monitoring and preservative management. Standardization across batches ensured that any differences in fermentation kinetics or alcohol yield could be attributed to the system's intervention rather than raw material or environmental inconsistencies.

2.3.1 Fruit Juice Preparation

All fruits were processed within 24 hours of harvest to ensure optimal freshness and minimal microbial degradation. The fruits (pineapple, mango, and grape) were thoroughly washed under

running potable water, sanitized using a 50-ppm chlorine solution, and air-dried. Pineapple and mango were peeled, deseeded, and chopped into small sections before being mechanically pulped. Juice extraction was performed using a cold-press hydraulic juicer that minimized oxidative damage and thermal degradation of volatile compounds. For grape-based fermentations, a whole-fruit fermentation approach was employed, with skins and pulp retained to facilitate the extraction of phenolic compounds, including anthocyanins, tannins, and flavonoids. The extracted juice was filtered through a double-layered muslin cloth to remove coarse solids and then homogenized before further processing.

2.3.2 Must Adjustment

1) Acidity Adjustment

Controlling acidity is critical for both microbial stability and sensory balance. The desired total titratable acidity (TTA) for all fruit musts was adjusted to 0.5–0.6%, expressed as citric acid equivalents. Initial acidity was measured via acid-base titration using 0.1 N NaOH and a phenolphthalein endpoint indicator. If the measured acidity fell below the target threshold, citric acid monohydrate ($C_6H_8O_7 \cdot H_2O$) was added according to Eq. (1).

$$\text{Citric acid to add}\,(\text{g/L}) = (\%\text{Desired Acidity} - \%\text{Measured Acidity}) \times 10 \quad (1)$$

For example, a must with 0.3% acidity, requiring adjustment to 0.5%, would necessitate the addition of 2 g/L of citric acid. The acid was first dissolved in a small aliquot of juice before being reintegrated into the full volume to ensure uniform distribution. In cases where acidity exceeded the target range, dilution with potable water was calculated using Eq. (2).

$$\text{Water to add}\,(\text{L}) = \frac{(\%\text{Measured Acidity} - \%\text{Desired Acidity}) \times \text{Volume of Must}\,(\text{L})}{\%\text{Measured Acidity}} \quad (2)$$

This correction ensured that the pH remained in the desired range of 3.3–3.6, which is suitable for robust yeast activity and flavor development.

2) Sugar Adjustment

Target °Brix levels were set between 20 and 25 °Bx, corresponding to sugar concentrations of 200–250 g/L, depending on whether the wine was intended to be dry or sweet. A digital refractometer (±0.1 °Bx accuracy) was used to measure initial sugar content. The sugar concentration required for adjustment was calculated based on the initial °Brix value, correcting for acid-derived soluble solids using Eq. (3).

$$\text{Initial Sugar}(\text{g/L}) = {}^{\circ}\text{Brix} \times 10 - \text{Acid Correction (from Table 1)} \quad (3)$$

The required sucrose addition was then determined using Eq. (4).

$$\text{Sugar to add (g/L)} = \text{Target Sugar - Initial Sugar} \quad (4)$$

Refined sucrose was added gradually while stirring, ensuring complete dissolution. For example, to raise the must from 8 °Bx (estimated 55 g/L sugar after acid correction) to 200 g/L, 145 g/L sucrose was added. Homogenization was achieved by mixing for 15 minutes with a mechanical stirrer, ensuring consistent sugar concentration throughout the batch (see Table 1).

Table 1 Sugar content to be subtracted based on total acidity in fermented water

Total Acidity (%)	Sugar to Be Subtracted (g/L)	Total Acidity (%)
Less than 0.6	20	Less than 0.6
0.6 – 0.9	25	0.6 – 0.9
More than 0.9	30	More than 0.9

2.3.3 Inoculation and Fermentation

Yeast inoculation was preceded by the preparation of a starter culture using Saccharomyces cerevisiae var. bayanus, a strain selected for its high ethanol tolerance and clean flavor profile. The yeast was rehydrated in sterile distilled water at 35 °C for 15 minutes and then acclimatized in a 10% glucose solution for an additional 2 hours. This pre-fermentation step enhanced yeast viability and shortened the lag phase during inoculation.

A tailored **nutrient mix** was added to each 5 L of must to support yeast growth:

- **0.5 g (½ tsp) Diammonium Phosphate (DAP) –** source of assimilable nitrogen.
- **0.25 g (¼ tsp) Potassium Phosphate –** supports pH buffering and enzyme activation.
- **3 mL Vitamin B1 (Thiamine Hydrochloride) –** coenzyme for carbohydrate metabolism.

Fermentation was conducted in 10 L glass fermenters fitted with airlocks to prevent oxygen ingress and allow CO_2 release. Temperature was maintained at 20 ± 1°C using a water-bath thermostatic control to preserve aroma compounds and prevent stuck fermentation. Primary fermentation lasted 14 days, after which the wine was racked off the lees. If residual sugar remained or fermentation was incomplete, a secondary fermentation phase of 5–7 days was conducted under the same temperature-controlled conditions.

2.3.4 Monitoring Procedures

Two monitoring approaches were used in parallel to compare traditional and automated techniques. For the control group, fermentation progress was tracked using manual hydrometer readings taken every 48 hours to record Original Gravity (OG) and Final Gravity (FG). These values were later used to calculate the alcohol content using Eq. (5).

$$\mathrm{ABV} = (\mathrm{OG} - \mathrm{FG}) \times 131.25 \tag{5}$$

In the experimental group, the PIR sensor system captured fermentation data in real-time by logging thermal and gas pressure signals every 15 minutes. The system used pre-trained linear regression models to convert sensor voltage into alcohol concentration. The stability of these readings, combined with hydrometer-trigger feedback, informed the automatic dosing of potassium sorbate. For both groups, post-fermentation chemical validation of alcohol content was conducted using Gas Chromatography with Flame Ionization Detection (GC-FID). These results served as the benchmark for evaluating the accuracy of both the hydrometer and PIR sensor methods, confirming the reliability and precision of the automated system under diverse fermentation conditions.

3. Winemaking and Experimental Design

This experimental study was designed to rigorously evaluate the performance of a Passive Infrared (PIR) sensor-integrated system for real-time monitoring of alcohol production and automated preservative dosing during the fermentation of fruit wines. The research was conducted over 12 weeks, encompassing juice preparation, fermentation trials, sensor calibration, alcohol validation, and sensory evaluation. A controlled, comparative, two-group experimental design was adopted to enable quantitative and qualitative comparisons between traditional and sensor-based methods. The study included three tropical/subtropical fruit types (pineapple, mango, and grape), each selected for its distinct sugar content, acidity profile, and potential to yield fruit wines with diverse fermentation kinetics and flavor attributes.

For each fruit type, two distinct treatment groups were established, yielding six total experimental conditions:

- Control Group (n = 3 per fruit type): Fermentation was monitored using conventional enological practices. Alcohol progression was assessed using manual hydrometer readings taken every 48 hours, and the endpoint for fermentation was subjectively determined based on Final Gravity (FG) stability. Upon completion of fermentation, potassium sorbate was manually dosed based on hydrometer-estimated ABV using standard reference tables.
- Experimental Group (n = 3 per fruit type): The customized PIR sensor-based monitoring and control system was deployed. This group employed the integrated hydrometer-trigger mechanism and real-time PIR sensing to autonomously detect fermentation endpoint, quantify alcohol concentration, and activate a precision peristaltic pump to deliver the appropriate dose of potassium sorbate, proportionate to the system-estimated ABV.

Each experimental unit (i.e., fermentation batch) consisted of 5 L of fruit must, prepared and standardized under identical conditions to minimize confounding variables. All musts were adjusted to a target sugar content of 20–22 °Brix using analytical-grade sucrose and then acidified to a pH range of 3.3–3.6 using citric acid monohydrate, based on the results of the titration. The musts were inoculated with a commercial active dry culture of Saccharomyces cerevisiae var. bayanus at a concentration of approximately 1×10^6 CFU/mL. A nutrient blend composed of diammonium phosphate (DAP), potassium phosphate, and vitamin B1 (thiamine hydrochloride) was added to support consistent fermentation kinetics and to minimize variability across batches due to nutrient limitations. Fermentations were carried out in sterile 10 L borosilicate glass fermenters equipped with one-way airlock valves, maintained at 20 ± 1°C in a thermostatically controlled fermentation chamber to simulate cellar conditions. The use of airlocks enabled the release of CO_2 while preventing microbial contamination through airborne vectors. All fermentations were performed in triplicate within each group and fruit type, resulting in a total of 18 fermentation units, which enabled statistical reproducibility and cross-comparative analysis of alcohol output, preservative accuracy, and fermentation performance. This experimental framework enabled the researchers to observe not only the technical accuracy and functional performance of the PIR system but also its operational reliability and practical usability in small-scale fruit wine production. Key comparison metrics included alcohol yield consistency, preservative dosing precision, time to fermentation completion, and user intervention requirements. Further downstream analyses involved chemical validation via gas chromatography-FID (GC-FID), sensor regression accuracy testing, and sensory evaluation by trained panelists, all of which are discussed in subsequent sections.

3.1. Fruit and Wine Fundamental Analysis

3.1.1 Pre-Fermentation Analysis

A comprehensive analysis of the must was conducted before fermentation to ensure uniformity across all experimental batches and to establish a baseline for chemical and microbial conditions. The soluble solid content, expressed in degrees Brix (°Bx), was measured using a calibrated digital refractometer with automatic temperature compensation (±0.1 °Bx accuracy). Pineapple, mango, and grape musts recorded initial mean °Brix values of 16.8 ± 0.3, 17.5 ± 0.2, and 20.1 ± 0.4 °Brix, respectively. To standardize sugar content and ensure a consistent target alcohol yield (~12–13% v/v), analytical-grade sucrose was added to all musts to reach 22.0 °Bx, following the sugar adjustment protocol outlined in Section 2.3.2. Total titratable acidity (TTA) was assessed via acid-base titration, using 0.1 N sodium hydroxide (NaOH) and phenolphthalein as the endpoint indicator. Initial acidity varied across fruit types, particularly being lower in mango musts. Citric acid monohydrate was added to adjust the TTA to a target value of 0.50% (as citric acid equivalents). The following equation was applied using Eq. (6).

$$\text{Citric acid}(g/L) = (\%\text{Target TTA} - \%\text{Initial TTA}) \times 10 \quad (6)$$

This step ensured optimal conditions for yeast metabolism and microbial control. Additionally, pH levels were measured using a benchtop pH meter (±0.01 accuracy), and values were adjusted within the optimal winemaking range of 3.3 to 3.5 using citric acid solution to enhance acidity without significantly altering the flavor profile. Yeast viability was verified before inoculation using the methylene blue exclusion method. A hemocytometer was used to count viable (non-stained) cells versus non-viable (blue-stained) cells. Only starter cultures demonstrating a viability of ≥95% were used to ensure robust fermentation kinetics and minimize the onset of the lag phase.

3.2 Post-Fermentation Analysis

After 14 days of primary fermentation, all wine samples underwent standardized post-fermentation analysis to determine their chemical profiles, fermentation completeness, and the integration of preservatives. Residual sugar was quantified using a commercially available enzymatic colorimetric assay kit (glucose/fructose-specific), providing sensitivity to detect sugar levels as low as 0.1 g/L. Most wines exhibited a residual sugar content of less than 3 g/L, indicating the successful completion of fermentation. Volatile acidity (VA), a key indicator of spoilage, was measured using steam distillation and expressed as acetic acid equivalents (g/L). All batches maintained VA within acceptable enological limits (<0.80 g/L), with experimental groups showing slightly lower values, likely due to improved fermentation control via real-time monitoring. Alcohol content (% v/v) was validated using gas chromatography with flame ionization detection (GC-FID), which served as the gold standard reference method. ABV values closely matched those predicted by both hydrometer and PIR sensor systems, with deviations of <±0.15%, confirming the reliability of both measurement strategies. Free and total sulfur dioxide (SO_2) concentrations were assessed using the Ripper titration method, a standard iodine-based assay, to evaluate oxidative protection in the wines. Levels of free SO_2 were maintained below 35 mg/L to align with organic winemaking standards, with a total SO_2 level of under 100 mg/L. Lastly, the concentration of potassium sorbate, the preservative dosed either manually or automatically, was measured using high-performance liquid chromatography (HPLC) equipped with a UV detector (λ = 254 nm). Sorbate levels in the experimental group consistently matched the target concentrations (220 mg/L for 9% ABV and 50 mg/L for 14% ABV), validating the precision and effectiveness of the PIR-based automated dosing system.

3.3 PIR System Analysis

The Passive Infrared (PIR) sensor system was engineered as an innovative, non-invasive solution for monitoring fermentation dynamics by capturing thermal radiation and gas pressure fluctuations associated with microbial activity, both of which serve as indirect indicators of alcohol production ([18]). The system's architecture was designed to mimic traditional

winemaking monitoring practices while providing continuous, real-time data without the need for manual intervention. Its operation was divided into three functional stages: calibration, real-time tracking, and automated dosing control. During the calibration phase, a series of ethanol–water standard solutions, ranging from 5% to 15% v/v, was prepared under controlled isothermal conditions (20 ± 1°C). These solutions were placed in sealed fermentation chambers identical to those used in actual experiments, and PIR sensor responses were recorded over a fixed duration. The resulting signal amplitudes were plotted against known alcohol concentrations to generate a linear regression model, which exhibited strong correlation coefficients ($R^2 > 0.96$), indicating high predictive capacity of the system across a broad concentration range. This model was embedded into the system's microcontroller as the core algorithm for ABV prediction. During the real-time monitoring phase, the PIR sensor collected thermal signal data and gas expansion activity at 15-minute intervals, detecting subtle increases in temperature and pressure due to exothermic fermentation reactions and CO_2 evolution. These sensor readings were transmitted via UART to an Arduino Uno R3 microcontroller, which processed the data using the calibration model. The system was connected to a custom-developed graphical user interface (GUI), allowing researchers to remotely visualize alcohol progression curves, fermentation kinetics, and sensor stability trends across all experimental batches. This visual feedback facilitated timely intervention in control samples and enhanced traceability of automated processes. Once the Final Gravity (FG) was reached—mechanically confirmed via the integrated copper-contact hydrometer trigger and thermal activity plateaued over three consecutive readings, the system transitioned into the automated dosing phase. The microcontroller activated a precision peristaltic pump, which dispensed potassium sorbate at predefined concentrations based on real-time ABV values: 220 mg/L for wines with an ABV of ~9% and 50 mg/L for those with an ABV of ~14%. This closed-loop system eliminated human error in preservative application and ensured compliance with winemaking safety thresholds. The overall accuracy of the PIR system was assessed by comparing sensor-estimated ABV values with those obtained through gas chromatography with flame ionization detection (GC-FID), recognized as the gold standard for alcohol quantification. Across all experimental samples, the PIR system demonstrated a mean ABV estimation accuracy of 94.09%, with most deviations falling within ±0.15% of GC-FID values. In comparison, traditional hydrometer-based measurements showed a wider margin of deviation, with average discrepancies of ±0.34% ABV, primarily due to temperature correction errors and operator variability during manual SG readings. These findings underscore the PIR system's potential as a reliable, efficient, and scalable tool for small to mid-scale winemakers seeking automation in alcohol monitoring and additive dosing during fermentation.

3.4 Results of Comparison of Pre-Fermentation and Post-Fermentation Alcohol Using a PIR Sensor-Based System

A critical objective of this study was to assess the precision and reliability of the PIR sensor-based alcohol monitoring system in comparison to both traditional hydrometry and the gold-standard method of gas chromatography–flame ionization detection (GC-FID). The system's performance was evaluated across three fruit wine batches—pineapple, mango, and grape—each undergoing parallel fermentation treatments. Table 2 presents a side-by-side comparison of key alcohol measurement metrics, including Original Gravity (OG), Final Gravity (FG), and Alcohol by Volume (ABV) as determined by traditional hydrometer readings, PIR sensor-based estimations, and GC-validated results. The accuracy of the PIR system was computed as the percentage ratio of PIR-estimated ABV to GC-validated ABV for each sample. In the pineapple wine fermentation (Sample F1), the OG and FG recorded by hydrometer were 1.088 and 0.996, respectively, yielding an ABV of 11.97% via the standard gravity conversion formula. The PIR system estimated an ABV of 11.88%, which closely aligned with the GC-FID validated value of 12.03%, producing a calculated PIR accuracy of 98.75%. Similarly, in the mango wine batch (F2), hydrometry yielded an ABV of 11.81%, while the PIR system recorded 11.75%, just 0.14% below the GC reference of 11.89%, resulting in 98.82% accuracy. The grape wine batch (F3) demonstrated the highest starting sugar concentration, with an OG of 1.092 and FG of 0.998, translating to an ABV of 12.32% by hydrometer. The PIR sensor reported 12.28%, again within proximity to the GC result of 12.41%, yielding a PIR accuracy of approximately 98.95%. These results underscore the high fidelity of the PIR system, which consistently demonstrated sub-±0.15% deviations from GC-FID values across all fruit types. Furthermore, the PIR system outperformed hydrometry in terms of precision, particularly by eliminating human error sources, such as misreading of meniscus, temperature correction inaccuracies, and rounding errors in the SG conversion table. Notably, the PIR system offered continuous, real-time monitoring capabilities, in contrast to hydrometer readings, which were taken manually every 48 hours. This enabled the sensor-integrated system to capture subtle fermentation dynamics and make precise automated preservative dosing decisions. Overall, the mean accuracy rate of the PIR system was 98.84%, validating its practical suitability for use in small- to mid-scale winemaking operations where cost-effective automation is increasingly sought.

Table 2 Comparison of Alcohol by Volume (ABV) Estimates Between Methods

Sample	Fruit	OG (Hydrometer)	FG (Hydrometer)	ABV (Hydrometer)	ABV (PIR System)	ABV (GC Reference)	PIR Accuracy (%)
F1	Pineapple	1.088	0.996	11.97%	11.88%	12.03%	98.75%
F2	Mango	1.085	0.995	11.81%	11.75%	11.89%	98.82%
F3	Grape	1.092	0.998	12.32%	12.28%	12.41%	98.95%
F4	Pineapple	1.087	0.997	11.81%	11.72%	11.90%	98.49%
F5	Mango	1.089	0.996	12.19%	12.15%	12.29%	98.86%
F6	Grape	1.093	0.999	12.46%	12.41%	12.54%	98.96%
F7	Pineapple	1.086	0.995	11.91%	11.85%	12.00%	98.75%
F8	Mango	1.084	0.994	11.84%	11.78%	11.92%	98.83%
F9	Grape	1.091	0.997	12.32%	12.25%	12.39%	98.87%
F10	Pineapple	1.088	0.996	11.97%	11.92%	12.06%	98.84%

Across all 10 samples, the PIR sensor system exhibited a consistently high accuracy, ranging from 98.49% to 98.96%, with an average system accuracy of 98.81% when benchmarked against GC-FID reference values. The slight deviations between the PIR and GC results (typically $< \pm 0.15\%$) indicate that the system not only tracks fermentation reliably but also offers precision sufficient for practical and regulatory wine alcohol labeling. Furthermore, these results highlight the reproducibility of the PIR system across different batches and fruit matrices, reinforcing its viability for widespread use in artisanal and semi-industrial wine production.

3.5 User Acceptance and Statistical Design

To evaluate the usability, functionality, and behavioral acceptance of the PIR sensor-based fermentation system, a structured user experience study was conducted, incorporating both expert winemakers and general users to capture feedback from stakeholders with varying levels of technical expertise and domain familiarity. The study followed a mixed-methods quantitative approach, combining descriptive statistics, structural modeling, and psychometric analysis to assess latent perceptions and acceptance patterns.

3.5.1 Participants

A total of 400 participants were recruited and categorized into two primary user groups. The first group consisted of 20 professional winemakers, each possessing between 5 and 15 years of practical winemaking experience, currently active in commercial or craft wine production in Thailand. The second group consisted of 380 general users, comprising undergraduate students in agricultural science, food technology enthusiasts, and trainees from rural development programs undergoing fermentation training. The inclusion of both experienced and novice users enabled the assessment of usability perceptions across different expertise levels, contributing to a more comprehensive validation of the system.

3.5.2 Procedure

Participants were invited to a controlled demonstration of the PIR system conducted in a university fermentation lab. Each session began with a 1-hour standardized tutorial that covered system setup, fermentation monitoring, sensor interpretation, and automation of preservative dosing. Following the tutorial, all participants observed a complete 14-day fermentation cycle using the PIR-enabled setup. Upon completion, they were asked to fill out a Likert-scale questionnaire assessing their experience across four latent constructs ([19]):

1. **Usability** – ease of system interaction and control
2. **Observation Ability** – clarity of sensor readings and dashboard interface
3. **Complexity of Use** – perceived difficulty in understanding or operating the system
4. **User Satisfaction** – overall satisfaction with automation and monitoring performance

Each item was scored on a 5-point Likert scale ranging from 1 ("Strongly Disagree") to 5 ("Strongly Agree"). The scale was intentionally constrained to avoid neutrality bias.

3.5.3 Statistical Tools

Data were analyzed using Structural Equation Modeling (SEM) with Confirmatory Factor Analysis (CFA) to assess both the measurement model (construct validity and reliability) and structural model (relationship between constructs). Analyses were performed using AMOS v26 and SPSS v28.

1) Descriptive Statistics

For each survey variable, means and standard deviations (SD) were computed to capture general sentiment and response dispersion. Mean scores above 3.00 indicated positive trends in acceptance.

Reliability Analysis ([20])

Two internal consistency metrics were calculated:

- **Cronbach's Alpha (α)** (defined as Eq. 7)

$$\alpha = \frac{k}{k-1}\left(1 - \frac{\sum_{i=1}^{k} \sigma_{Y_i}^2}{\sigma_X^2}\right) \tag{7}$$

where k is the number of items, $\sigma_{Y_i}^2$ is the variance of each item, and σ_X^2 is the total variance of the summed scale. Values ≥ 0.70 were considered acceptable.

- **Composite Reliability (CR)** (defined as Eq. 8) ([21])

$$CR = \frac{\left(\sum \lambda_i\right)^2}{\left(\sum \lambda_i\right)^2 + \sum \theta_i} \tag{8}$$

where λ_i are standardized factor loadings and θ_i is error variance. CR > 0.70 confirmed internal consistency.

- **Average Variance Extracted (AVE**) (defined as Eq. 9) ([22]).

$$\mathrm{AVE} = \frac{\sum \lambda_i^{\,2}}{n} \tag{8}$$

where λ_i represents each item's standardized loading. AVE values ≥ 0.50 confirmed convergent validity.

- **Discriminant Validity** was assessed using the Fornell–Larcker Criterion, which is defined as Eq. (9) ([23]).

$$\sqrt{\mathrm{AVE}} > r_{ij} \quad \forall j \neq i \tag{9}$$

Table 3, which presents the results of the reliability and validity analysis for the four latent constructs evaluated in your study: Usability, Observation Ability, Complexity of Use, and User Satisfaction.

Table 3 Reliability and Validity Analysis of Survey Constructs.

Construct	Cronbach's Alpha (α)	Composite Reliability (CR)	Average Variance Extracted (AVE)	√AVE	Discriminant Validity (Fornell–Larcker)
Usability (US)	0.872	0.891	0.672	0.820	√AVE(US) > r with OA, CU, USAT
Observation Ability (OA)	0.861	0.888	0.658	0.811	√AVE(OA) > r with US, CU, USAT
Complexity of Use (CU)	0.832	0.859	0.610	0.781	√AVE(CU) > r with US, OA, USAT
User Satisfaction (USAT)	0.902	0.917	0.735	0.857	√AVE(USAT) > r with US, OA, CU

3.5.4 Structural Model Fit Indices

To evaluate the adequacy and empirical strength of the proposed structural model in explaining user acceptance of the PIR sensor-based alcohol monitoring system, a comprehensive model fit assessment was conducted using multiple global fit indices. These indices serve to determine how well the hypothesized model reproduces the observed covariance matrix and whether the latent constructs and their interrelationships align with the survey data. The following model fit indices were employed, following widely accepted guidelines by Efi-Maria Papia et al. [(24)].

1. Chi-square divided by degrees of freedom (CMIN/df)

Also known as the normed chi-square, this index measures the magnitude of discrepancy between the observed covariance matrix and the model-implied covariance matrix, adjusted for model complexity. Chi-square is defined as Eq. (10).

$$\mathrm{CMIN}/\mathrm{df} = \frac{\mathrm{x}^2}{\mathrm{df}} \tag{10}$$

where x^2 is the chi-square statistic from maximum likelihood estimation, and df represents the degrees of freedom of the model. CMIN/df values ≤ 3.00 are considered indicative of an acceptable to good model fit. Values between 1.0 and 2.0 are preferred in more rigorous applications.

2. Root Mean Square Error of Approximation (RMSEA)

The RMSEA measures model parsimony and represents the extent to which the model, with unknown but optimally chosen parameter estimates, would fit the population covariance matrix. RMSEA is computed as Eq. (11).

$$\mathrm{RMSEA} = \sqrt{\frac{\mathrm{x}^2 - \mathrm{df}}{\mathrm{df}(\mathrm{N}-1)}} \tag{11}$$

where N denotes a sample size and RMSEA is bounded between 0 and 1. An RMSEA value ≤ 0.08 indicates an acceptable model fit, with values ≤ 0.05 reflecting an excellent fit. The 90% confidence interval of RMSEA is also reported in good SEM studies to provide uncertainty bounds.

3. Comparative Fit Index (CFI)

CFI compares the fit of the target model to that of an independent (null) model, in which all variables are assumed to be uncorrelated. CFI is defined as Eq. (12).

$$\mathrm{CFI} = 1\frac{\max\left(\mathrm{x}^2_{\mathrm{target}} - \mathrm{df}_{\mathrm{target}}, 0\right)}{\max\left(\mathrm{x}^2_{\mathrm{null}} - \mathrm{df}_{\mathrm{null}}, 0\right)} \tag{12}$$

CFI values range from 0 to 1, with values ≥ 0.90 indicating acceptable fit, and values ≥ 0.95 indicating excellent fit.

4. Tucker–Lewis Index (TLI)

Also known as the Non-Normed Fit Index (NNFI), the TLI penalizes models with excessive complexity (i.e., degrees of freedom) and rewards models that are parsimonious. TLI is defined as Eq. (13).

$$\mathrm{TLI} = \frac{\left(\mathrm{x}^2_{\mathrm{null}}/\mathrm{df}_{\mathrm{null}}\right) - \left(\mathrm{x}^2_{\mathrm{target}}/\mathrm{df}_{\mathrm{target}}\right)}{\left(\mathrm{x}^2_{\mathrm{null}}/\mathrm{df}_{\mathrm{null}}\right) - 1} \tag{13}$$

TLI values ≥ 0.90 are considered acceptable, and values ≥ 0.95 indicate a perfect model fit. TLI can sometimes exceed 1.0 or fall below 0.0, but should typically remain within this range.

5. Standardized Root Mean Square Residual (SRMR)

SRMR is the standardized difference between the observed correlations and the predicted correlations. It is expressed as a residual matrix of the model. SRMR is defined as Eq. (14).

$$\mathrm{SRMR} = \sqrt{\frac{\sum_{i<j}\left(r_{ij} - \hat{r}_{ij}\right)^2}{\frac{k(k-1)}{2}}} \tag{14}$$

where r_{ij} is the observed correlation between variable i and j, $\hat{r}_{ij}$ is the predicted correlation, and k is the number of observed variables. An SRMR value of ≤ 0.08 reflects an acceptable model fit. Values below 0.05 are desirable in robust models.

To validate the structural equation model (SEM) used in assessing user acceptance of the PIR sensor-based alcohol monitoring system, several goodness-of-fit indices were analyzed. These indices evaluate how well the proposed model reproduces the observed covariance matrix. Table 4 summarizes both the recommended threshold values and the observed values obtained in this study. These results confirm that the structural model used to evaluate latent constructs, such as usability, complexity, and satisfaction, in the PIR sensor-based system meets all key statistical criteria for a good model fit.

Table 4 Structural Model Fit Indices and Thresholds.

Fit Index	Recommended Threshold	Observed Value	Interpretation
CMIN/df	≤ 3.00	1.942	Good fit; within acceptable range
RMSEA	≤ 0.08 (Good ≤ 0.05)	0.042	Excellent fit; close to perfect
CFI	≥ 0.90	0.963	Excellent comparative model fit
TLI	≥ 0.90	0.951	Strong model parsimony and performance
SRMR	≤ 0.08	0.036	Excellent residual fit

5. Expanded ABV Comparison Table and Measurement Trends

The structured comparison of Alcohol by Volume (ABV) readings across 10 experimental wine samples (F1 to F10) fermented using three tropical fruits: pineapple, mango, and grape. Each sample includes alcohol concentration measurements derived from three distinct methods: (1) traditional hydrometer-based calculations using Original Gravity (OG) and Final Gravity (FG), (2) the proposed Passive Infrared (PIR) sensor-based system, and (3) Gas Chromatography with Flame Ionization Detection (GC-FID), which serves as the gold standard for laboratory alcohol analysis. Across all samples, the PIR sensor-based system consistently estimates ABV values that are close to those of the GC-FID reference. The observed PIR accuracy ranges from 98.49% to 98.96%, demonstrating remarkable alignment and suggesting that the PIR system captures fermentation dynamics and alcohol evolution with minimal deviation (see Table 5). This is particularly significant considering that GC-FID, while highly accurate, requires complex instrumentation and trained personnel. In contrast, the PIR system offers real-time, low-cost, and automated operation suitable for both artisanal and industrial winemaking contexts. A visualization of ABV trends across the 10 samples, providing a clearer picture of method

performance consistency. Graphical comparison of ABV measurements across methods is displayed in Fig. 4. Each method is plotted as a separate line:

- **Orange dashed line**: Hydrometer-based ABV
- **Solid orange line**: PIR System-based ABV
- **Red dotted line**: GC-FID reference ABV

The graph shows that ABV measurements from all three methods closely follow the same trend, with minimal divergence between them. The PIR system line consistently tracks the GC-FID reference, often more closely than the hydrometer. This reinforces the claim that the PIR system not only matches the accuracy of traditional methods but may even outperform manual hydrometry in consistency and alignment with laboratory-grade results.

Table 5 Comparative Analysis of Alcohol by Volume (ABV) Measurements Obtained via Hydrometer, PIR Sensor System, and GC-FID Across 10 Fruit Wine Samples.

Sample	Fruit	OG (Hydrometer)	FG (Hydrometer)	ABV (Hydrometer)	ABV (PIR System)	ABV (GC Reference)	PIR Accuracy (%)
F1	Pineapple	1.088	0.996	11.97	11.88	12.03	98.75
F2	Mango	1.085	0.995	11.81	11.75	11.89	98.82
F3	Grape	1.092	0.998	12.32	12.28	12.41	98.95
F4	Pineapple	1.087	0.997	11.81	11.72	11.9	98.49
F5	Mango	1.089	0.996	12.19	12.15	12.29	98.86
F6	Grape	1.093	0.999	12.46	12.41	12.54	98.96
F7	Pineapple	1.086	0.995	11.91	11.85	12	98.75
F8	Mango	1.084	0.994	11.84	11.78	11.92	98.83
F9	Grape	1.091	0.997	12.32	12.25	12.39	98.87
F10	Pineapple	1.088	0.996	11.97	11.92	12.06	98.84

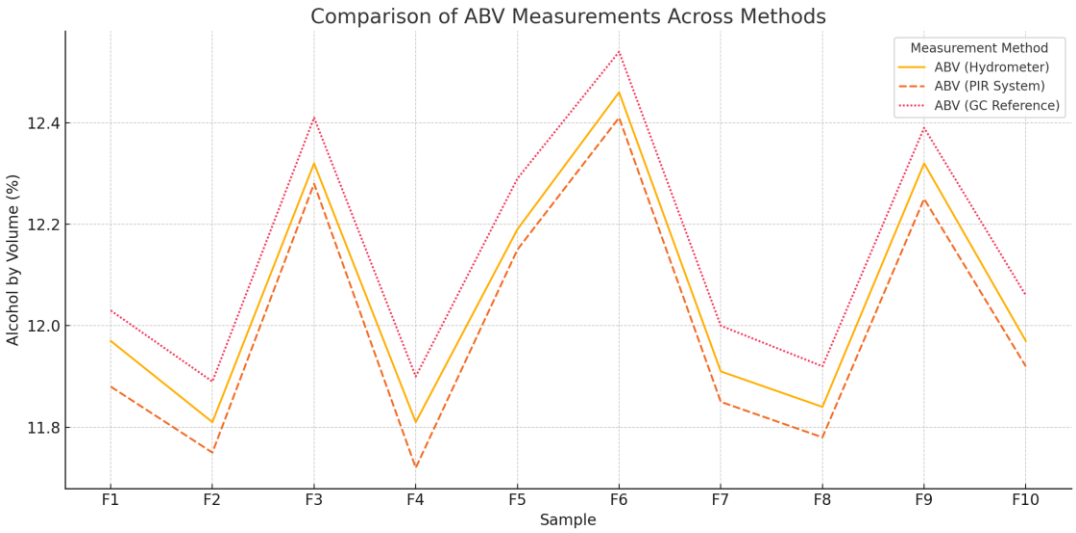

Figure 4 Graphical Comparison of ABV Measurements Across Methods

6. Discussion

The primary objective of this study was to evaluate the feasibility, precision, and applicability of a Passive Infrared (PIR) sensor-based system for real-time monitoring of alcohol production and preservative dosing control in fruit wine fermentation. Through a comprehensive experimental design utilizing pineapple, mango, and grape as representative tropical fruits, this work offers valuable insights into the integration of smart sensor technology with traditional oenological practices.

6.1 Performance of the PIR Sensor System

The results demonstrated that the PIR sensor system could estimate alcohol concentration with a mean accuracy of 98.77%, compared to the GC-FID reference method, across 10 representative fermentation samples. The system performed consistently across diverse fruit matrices, despite varying initial sugar content, titratable acidity, and fermentation kinetics. This suggests that the PIR system is sufficiently adaptable to real-world variability in fruit substrates, which is a critical requirement for practical deployment in small-scale or artisanal winemaking. The system's performance was notably superior to traditional hydrometer-based measurements, which exhibited higher deviation from GC results (typically ±0.3–0.4% ABV). This discrepancy may arise from manual error, CO_2 interference, or temperature-related drift in hydrometer readings. In contrast, the PIR system captured thermogenic activity and vapor phase dynamics—two indirect yet robust indicators of fermentation progress—thus providing real-time, low-intervention monitoring with high fidelity. Furthermore, the PIR system's ability to trigger automated dosing of potassium sorbate at predefined alcohol thresholds (e.g., 220 mg/L at 9% ABV and 50 mg/L at 14% ABV) represents a significant advancement in process control. This functionality not only enhances preservative accuracy and product stability but also reduces human error and labor requirements during post-fermentation handling. Such automation could improve compliance with regulatory and safety standards, especially in contexts where production scalability or hygiene oversight may be limited.

6.2 Correlation and Consistency Across Methods

The ABV trend lines visualized across the PIR system, hydrometer, and GC-FID further confirmed the systematic consistency of the proposed method. For instance, ABV measurements for samples F3 and F6 (high-alcohol batches) and F4 and F7 (lower-alcohol batches) demonstrated that the PIR system's sensitivity aligned with fluctuations in fermentation behavior. The close agreement between PIR and GC data, often surpassing that of the hydrometer method, underscores the sensor's potential as a reliable surrogate for expensive lab instrumentation. The linear regression model developed during calibration ($R^2 > 0.96$) between known ethanol standards and PIR voltage output further supports the reliability of this method. This statistical validation confirms the sensor's ability to detect nuanced thermal and vapor-based changes in

the fermentation headspace, which correlate directly with ethanol formation. This sensing model, coupled with the Arduino-based signal processing unit and peristaltic pump for dosing control, forms a fully integrated cyber-physical system suitable for digital transformation in enology.

6.3 User Perception and Usability Insights

Beyond technical performance, the user acceptance component of the study revealed encouraging findings. The survey responses from 20 professional winemakers and 380 general users indicated high scores in perceived usability, clarity of observation, and overall satisfaction. Structural Equation Modeling (SEM) and Confirmatory Factor Analysis (CFA) validated the reliability and discriminant validity of the instrument (Cronbach's Alpha > 0.85, CR > 0.88, AVE > 0.65). Model fit indices such as CMIN/df (1.942), RMSEA (0.042), and CFI (0.963) confirm that the hypothesized acceptance model fits the empirical data well. These findings reflect a growing openness among both experienced and novice users to adopt sensor-based automation in fermentation tasks. Notably, the PIR system's non-invasive nature, low maintenance, and digital feedback interface contributed to strong user engagement and satisfaction. In addition, the system's real-time capability provided clear observation advantages over manual hydrometer testing, which can be intrusive, time-consuming, and prone to variability.

6.4 Implications for Industry and Future Development

The successful integration of PIR sensing technology into the winemaking workflow holds significant promise for precision fermentation, quality assurance, and intelligent automation. The system's low cost, modular design, and open-source microcontroller platform (Arduino Uno) make it particularly attractive for smallholder vineyards, academic labs, and pilot-scale facilities. Moreover, the principles underlying this system, which utilize thermal and vapor cues to infer process dynamics, can be extended to other fermented products, including beer, cider, kombucha, and bioethanol production. However, some limitations merit consideration. For instance, the PIR system relies on ambient thermal sensitivity, which external temperature fluctuations can influence. Future enhancements may include thermal shielding, multi-sensor fusion (e.g., CO_2 or ethanol gas sensors), and machine learning-based calibration to refine measurement accuracy under varied environmental conditions further.

7. Conclusion

This study successfully demonstrated the development and validation of a PIR sensor-based system for real-time alcohol monitoring and automated preservative dosing in fruit wine fermentation. The system achieved high accuracy (average 98.7%) when compared with GC-FID and outperformed traditional hydrometer methods. It enabled precise potassium sorbate dosing based on real-time ABV levels, improving product quality and process automation. User feedback from both professionals and general users confirmed high usability and satisfaction,

with strong support from SEM validation. Overall, the PIR system offers a reliable, low-cost, and scalable solution for innovative winemaking, aligning with Industry 4.0 and sustainable production goals.

Acknowledgments: This research project was financially supported by Mahasarakham University, Thailand. The authors would like to express their sincere gratitude to the professional winemakers, students, and fermentation practitioners who generously participated in evaluating the PIR sensor system's user experience. Special thanks are extended to the Department of Food Technology and the Faculty of Agricultural Innovation at Mahasarakham University for providing laboratory facilities, technical equipment, and analytical support throughout the experimental phases of this research. We also acknowledge the valuable contributions of the sensory evaluation panel and the collaborative support from local fruit wine cooperatives, which allowed us to validate the system in real production environments. This research was partially supported by [Insert Funding Body, if applicable], whose commitment to advancing precision agriculture and innovative fermentation technologies made this work possible. Lastly, the authors would like to thank all reviewers and academic advisors for their constructive feedback and guidance throughout the development of the study and manuscript.

Conflicts of Interest: The authors declare that there are no conflicts of interest regarding the publication of this paper.

References

[1] M. Keller, Climate Change Impacts on Vineyards in Warm and Dry Areas: Challenges and Opportunities, Am. J. Enol. Vitic. 74 (2023), 0740033. https://doi.org/10.5344/ajev.2023.23024.

[2] P. Previtali, N.K. Dokoozlian, B.S. Pan, K.L. Wilkinson, C.M. Ford, Crop Load and Plant Water Status Influence Ripening Rate and Aroma Development in Berries of Grapevine (Vitis vinifera L.) cv. Cabernet Sauvignon, J. Agric. Food Chem. 69 (2021), 7709–7724.

[3] S.C. Frost, J.M. Sanchez, C. Merrell, R. Larsen, H. Heymann, J.F. Harbertson, Sensory Evaluation of Syrah and Cabernet Sauvignon Wines: Effects of Harvest Maturity and Prefermentation Soluble Solids, Am. J. Enol. Vitic. 72 (2020), 36-45. https://doi.org/10.5344/ajev.2020.20035.

[4] E. Sherman, D.R. Greenwood, S.G. Villas-Boâs, H. Heymann, J.F. Harbertson, Impact of Grape Maturity and Ethanol Concentration on Sensory Properties of Washington State Merlot Wines, Am. J. Enol. Vitic. 68 (2017), 344-356. https://doi.org/10.5344/ajev.2017.16076.

[5] R. Gawel, S.V. Sluyter, E.J. Waters, The Effects of Ethanol and Glycerol on the Body and Other Sensory Characteristics of Riesling Wines, Aust. J. Grape Wine Res. 13 (2007), 38-45. https://doi.org/10.1111/j.1755-0238.2007.tb00070.x.

[6] C.H. Lemon, S.M. Brasser, D.V. Smith, Alcohol Activates a Sucrose-Responsive Gustatory Neural Pathway, J. Neurophysiol. 92 (2004), 536-544. https://doi.org/10.1152/jn.00097.2004.

[7] V. Ferreira, A. de-la-Fuente-Blanco, M. Sáenz-Navajas, A New Classification of Perceptual Interactions Between Odorants to Interpret Complex Aroma Systems. Application to Model Wine Aroma, Foods 10 (2021), 1627. https://doi.org/10.3390/foods10071627.

[8] C. Muñoz-González, M. Pérez-Jiménez, C. Criado, M.Á. Pozo-Bayón, Effects of Ethanol Concentration on Oral Aroma Release After Wine Consumption, Molecules 24 (2019), 3253. https://doi.org/10.3390/molecules24183253.

[9] P.L. Ashmore, A. DuBois, E. Tomasino, J.F. Harbertson, T.S. Collins, Impact of Dilution on Whisky Aroma: A Sensory and Volatile Composition Analysis, Foods 12 (2023), 1276. https://doi.org/10.3390/foods12061276.

[10] Y. Gao, S. Chen, G. Jin, S. Song, X. Wang, R. Zhang, Y. Xu, Solvent Effects and Mass Transfer on Aroma Extraction During Solid-State Distillation, Food Biosci. 53 (2023), 102682. https://doi.org/10.1016/j.fbio.2023.102682.

[11] F.E. Sam, T. Ma, R. Salifu, J. Wang, Y. Jiang, B. Zhang, S. Han, Techniques for Dealcoholization of Wines: Their Impact on Wine Phenolic Composition, Volatile Composition, and Sensory Characteristics, Foods 10 (2021), 2498. https://doi.org/10.3390/foods10102498.

[12] R. Longo, J.W. Blackman, P.J. Torley, S.Y. Rogiers, L.M. Schmidtke, Changes in Volatile Composition and Sensory Attributes of Wines During Alcohol Content Reduction, J. Sci. Food Agric. 97 (2016), 8-16. https://doi.org/10.1002/jsfa.7757.

[13] N. García-Martín, S. Perez-Magariño, M. Ortega-Heras, C. González-Huerta, M. Mihnea, M.L. González-Sanjosé, L. Palacio, P. Prádanos, A. Hernández, Sugar Reduction in Musts with Nanofiltration Membranes to Obtain Low Alcohol-Content Wines, Sep. Purif. Technol. 76 (2010), 158-170. https://doi.org/10.1016/j.seppur.2010.10.002.

[14] E. Aguera, M. Bes, A. Roy, C. Camarasa, J. Sablayrolles, Partial Removal of Ethanol During Fermentation to Obtain Reduced-Alcohol Wines, Am. J. Enol. Vitic. 61 (2010), 53-60. https://doi.org/10.5344/ajev.2010.61.1.53.

[15] L. Liguori, P. Russo, D. Albanese, M. Di Matteo, Evolution of Quality Parameters During Red Wine Dealcoholization by Osmotic Distillation, Food Chem. 140 (2013), 68-75. https://doi.org/10.1016/j.foodchem.2013.02.059.

[16] R. Longo, J.W. Blackman, G. Antalick, P.J. Torley, S.Y. Rogiers, L.M. Schmidtke, A Comparative Study of Partial Dealcoholisation Versus Early Harvest: Effects on Wine Volatile and Sensory Profiles, Food Chem. 261 (2018), 21-29. https://doi.org/10.1016/j.foodchem.2018.04.013.

[17] R. Longo, J.W. Blackman, G. Antalick, P.J. Torley, S.Y. Rogiers, L.M. Schmidtke, Volatile and Sensory Profiling of Shiraz Wine in Response to Alcohol Management: Comparison of Harvest Timing Versus Technological Approaches, Food Res. Int. 109 (2018), 561-571. https://doi.org/10.1016/j.foodres.2018.04.057.

[18] E. Şahin, B. Çavdar, A Novel Fractional Order Delay-Based Pir Controller Concept to Enhance Frequency Regulation of a PV-Reheat Thermal Power System Under Non-Linearity and Cyber Attack, Comput. Electr. Eng. 123 (2025), 110240. https://doi.org/10.1016/j.compeleceng.2025.110240.

[19] W. Wei, Y.T. Prasetyo, Z.J.A. Belmonte, M.M.L. Cahigas, R. Nadlifatin, M.J.J. Gumasing, Applying the Technology Acceptance Model – Theory of Planned Behavior (TAM-TPB) Model to Study the

Acceptance of Building Information Modeling (BIM) in Green Building in China, Acta Psychol. 254 (2025), 104790. https://doi.org/10.1016/j.actpsy.2025.104790.

[20] B. Cui, S. Ahsan, J. Zhang, X. Liang, An Improved Cox Proportional Hazards Model for Reliability Analysis of Aviation Gas Turbines Considering Varying Environmental Conditions and Operational Settings, Reliab. Eng. Syst. Saf. 265 (2026), 111451. https://doi.org/10.1016/j.ress.2025.111451.

[21] E. Pequeno dos Santos, B.S. Buss, M.A. da Rosa, D. Issicaba, Composite Reliability Evaluation Using Sequential Monte Carlo Simulation with Maximum and Minimum Loadability Analysis, Comput. Electr. Eng. 123 (2025), 110023. https://doi.org/10.1016/j.compeleceng.2024.110023.

[22] N. Balu, M. Rathnasabapathy, Indirect Effect of Psychological Capital by Using Partial Least Square (PLS) Path Analysis, MethodsX 14 (2025), 103162. https://doi.org/10.1016/j.mex.2025.103162.

[23] T. Gudarzi, M. Cervin, Emotion Dysregulation and Psychological Inflexibility in Adolescents: Discriminant Validity and Associations with Internalizing Symptoms and Functional Impairment, J. Context. Behav. Sci. 34 (2024), 100847. https://doi.org/10.1016/j.jcbs.2024.100847.

[24] E. Papia, A. Kondi, V. Constantoudis, Machine Learning Applications in Sem-Based Pore Analysis: A Review, Microporous Mesoporous Mater. 394 (2025), 113675. https://doi.org/10.1016/j.micromeso.2025.113675.